



# Speed skills: measuring the visual speed analyzing properties of primate MT neurons

John A. Perrone<sup>1</sup> and Alexander Thiele<sup>2,3</sup>

<sup>1</sup> Department of Psychology, The University of Waikato, Private Bag 3105, Hamilton, New Zealand

<sup>2</sup> The Salk Institute for Biological Studies, 10010 N. Torrey Pines Rd., La Jolla, California 92037, USA

<sup>3</sup> Present address: Department of Psychology, University of Newcastle upon Tyne, Ridley Building, Claremont Place, Newcastle upon Tyne, NE1 7RU, UK

Correspondence should be addressed to J.P. ([jpnz@waikato.ac.nz](mailto:jpnz@waikato.ac.nz))

Knowing the direction and speed of moving objects is often critical for survival. However, it is poorly understood how cortical neurons process the speed of image movement. Here we tested MT neurons using moving sine-wave gratings of different spatial and temporal frequencies, and mapped out the neurons' spatiotemporal frequency response profiles. The maps typically had oriented ridges of peak sensitivity as expected for speed-tuned neurons. The preferred speed estimate, derived from the orientation of the maps, corresponded well to the preferred speed when moving bars were presented. Thus, our data demonstrate that MT neurons are truly sensitive to the object speed. These findings indicate that MT is not only a key structure in the analysis of direction of motion and depth perception, but also in the analysis of object speed.

For most species, the analysis of visual motion is essential for extracting information about the surrounding environment<sup>1,2</sup>. Knowing what direction and how fast something moves is often critical for capturing prey and for avoiding capture. Visual motion information also aids in the perceptual reconstruction of the spatial layout of the environment around us as we navigate through the world<sup>3–5</sup>. Neurons in the middle temporal (MT) area of primate visual cortex are specialized for visual motion extraction<sup>6,7</sup>. Research on the MT neurons' properties has largely concentrated on examining how they encode the direction of moving features (for example, refs. 8–11)—much less is known about how they process the speed of image movement.

The visual speed signals from area MT have been implicated in a number of important behavioral tasks, such as the visual pursuit of moving targets<sup>12,13</sup> and the determination of self-motion<sup>5,14</sup>. Understanding the speed-tuning characteristics of MT neurons is therefore crucial for determining how the brain performs these tasks. The speed tuning of MT neurons has been assessed using moving bars or random dot patterns across a range of speeds<sup>15–18</sup>, and the resulting tuning curves were often quite peaked<sup>15</sup>. This was taken as evidence that these neurons are tuned for the speed of image motion.

However, the possibility remains that MT neurons are tuned to the temporal frequency of changes in the light intensity pattern rather than specifically to the speed of the moving feature. Consider, for example, neurons in the primate primary visual cortex (V1). If tested with a moving bar or edge, some primate V1 neurons will respond more strongly to a particular speed of the bar/edge<sup>19</sup>, so one could mistakenly conclude that these neurons are speed tuned. However, the response of these V1 neurons also depends on the spatial structure of the stimulus (the spatial frequency); they are not uniquely responding to the image speed<sup>20</sup>.

Changes to either the spatial or temporal frequency will influence their firing rates. A neuron truly encoding image speed will respond to a particular speed, regardless of the spatial frequency content in the stimulus. It is currently not clear whether MT neurons have this property, although preliminary evidence suggests that some may fit in this category (W.T. Newsome, M.S. Gizzi & J.A. Movshon, *Invest. Ophthalm. Vis. Sci. Suppl.* **24**, 106, 1983; J.A. Movshon *et al.*, *Invest. Ophthalm. Vis. Sci. Suppl.* **29**, 327, 1988).

The analysis and understanding of visual motion stimuli can benefit from a transformation into the spatiotemporal or frequency domain<sup>21</sup>. Moving edges are a common part of our visual environment and can be analyzed in terms of their spatial and temporal frequency content. According to Fourier theory<sup>22</sup>, a static edge can be synthesized from a combination of two-dimensional intensity sine-wave components (Fig. 1a and b). Because the edge is not moving, all the different sinusoids have temporal frequencies of 0 Hz. In a plot of spatial frequency versus temporal frequency (Fig. 1c), the amplitude spectrum for this static edge would fall on a horizontal line at 0 Hz.

When the edge moves from right to left at a particular speed  $v$ , the low-frequency sine-wave components of the edge will have a low temporal frequency. However, to 'keep in step,' the high spatial frequency components will necessarily have a high temporal frequency<sup>23</sup>. An edge moving leftward at speed  $v$  will therefore have a spectrum with a slope equal to  $v$  when plotted in spatiotemporal frequency space (Fig. 1c)<sup>21,24</sup>. The spectrum necessarily passes through (0, 0). The overall speed of each sine-wave component is equal to the temporal frequency divided by the spatial frequency. If the speed of the edge increases, the spatial frequency content remains the same, but the temporal frequency of each component increases by an amount proportional to the spatial frequency, and thus, the

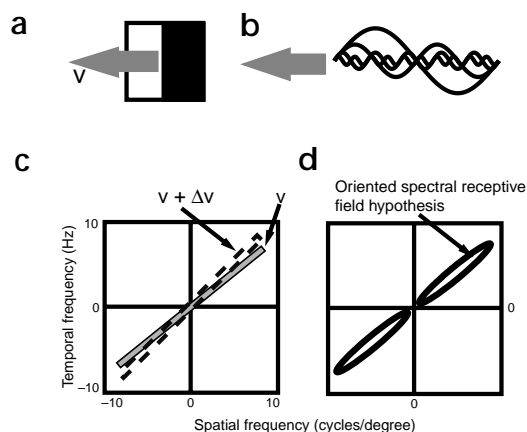


**Fig. 1.** Representation of a moving edge in the spatiotemporal frequency domain. (a) Edge moving from right to left at speed  $v$  (degrees/s). (b) Stylized Fourier sine-wave components making up the edge profile. The different sinusoids generate different temporal frequencies, because the temporal frequency is a product of the speed ( $v$ ) and the spatial frequency of the sinusoid. High spatial frequency sinusoids will have higher temporal frequencies than the low spatial frequency sinusoids. (c) Spatial versus temporal frequency plot, with the shaded line representing the Fourier amplitude spectrum of the moving edge. The length of the line has been truncated to better indicate changes to its position. The spectrum has a slope equal to  $v$  and passes through  $(0, 0)$ . If the speed of the edge increases by  $\Delta v$ , the temporal frequency of each sinusoid increases by an amount proportional to the spatial frequency. This results in a change in the slope or orientation of the spectrum (dashed lines). (d) A mechanism sensitive to particular orientations of the edge spectrum (that is, the speed) would be expected to have a region of peak sensitivity that is elongated and oriented relative to the spatial and temporal frequency axes.

slope of the edge spectrum increases (Fig. 1c). Therefore, any neural mechanism (either a single sensor or an ensemble) encoding the particular speed  $v$  of the moving edge needs to respond selectively to the slope of the edge spectrum.

Such a mechanism would respond best to combinations of spatial and temporal frequencies that fall along a straight line in frequency space (Fig. 1d). This mechanism would respond equally well to sine-wave gratings of various spatiotemporal frequency content as long as the speed of the sine wave was equal to  $v$ . The sensitivity profile of the mechanism in the spatiotemporal frequency domain will be referred to as the 'spectral receptive field.' The spectral receptive field is the amplitude part of the Fourier-transformed spatiotemporal receptive field, and it gives an indication as to which spatial and temporal frequencies will cause the mechanism to respond. We will refer to the hypothetical speed-tuned mechanism as the 'oriented spectral receptive field hypothesis.' Such oriented mechanisms are often referred to as being 'inseparable' because one cannot generate them by simply multiplying together two separate spatial and temporal frequency amplitude response functions.

If MT neurons are truly speed tuned, they should possess spectral receptive fields that are oriented relative to the spatial and temporal frequency axes. Moreover, one should find a range of spectral receptive field orientations, each corresponding to the preferred speed of the individual MT neuron<sup>15–18</sup>. The main goal of this study was to look for any sign of orientation. We therefore mapped out the spectral receptive fields of MT neurons to look for evidence of oriented (inseparable) spectral receptive fields. Such evidence would confirm that these neurons are truly sensitive to the speed of moving edges and are not just responding to the temporal frequency component of the motion. We found that a large proportion of our MT neurons had oriented (inseparable) spectral receptive fields, and that this orientation was closely linked to a neuron's speed tuning when tested with a moving bar.

## RESULTS

### Inseparable versus separable spectral receptive fields

Contour plots (Fig. 2) from four representative MT neurons in our sample ( $n = 84$ ) exhibit regions of peak sensitivity that are

clearly oriented relative to the spatial and temporal frequency axes. Therefore, these data support the oriented spectral receptive field hypothesis. To quantify the degree of orientation in all of our cells, we fitted the 30 grating responses using two different types of two-dimensional Gaussian functions: non-oriented and oriented (see Methods). The latter included an extra parameter, which rotated the Gaussian around its peak by an angle  $\theta$  measured relative to the vertical. The non-oriented fit function is equivalent to the oriented function when  $\theta = 0^\circ$ . In both cases, the best fit between the particular Gaussian and the MT-normalized responses (for example, Fig. 3) was carried out using least-squares minimization (see Methods).

The correlation coefficient ( $r$ ) was calculated as an overall measure of the degree of fit. In Fig. 3, the non-oriented fit and oriented fit  $r$ -values were 0.75 and 0.88, respectively. Across our whole population, the means  $\pm$  s.d. of the  $r$ -values for the non-oriented and oriented fits were  $0.80 \pm 0.13$  and  $0.86 \pm 0.10$ , respectively. For each cell, we tested the hypothesis that the  $\theta$  parameter in the oriented-fit model was  $0^\circ$ , using a non-linear regression analysis that generates a Student  $t$ -statistic<sup>25</sup> (see Methods). A significant  $t$ -value indicated that we could reject the hypothesis that the  $\theta$  parameter value is  $0^\circ$ .

For the neuron in Fig. 3, the  $t$ -value was 5.9, which exceeded the critical value,  $t = 2.06$  ( $24 df$ ,  $p < 0.005$ , two-tailed). Thus, for this neuron, we could reject the hypothesis  $H_0: \theta = 0^\circ$ . For our population of MT neurons, the mean  $t$ -value was  $3.12 \pm 3.3$  (s.d.), and the median was 2.59. Most (61%) neurons generated  $t$ -values that

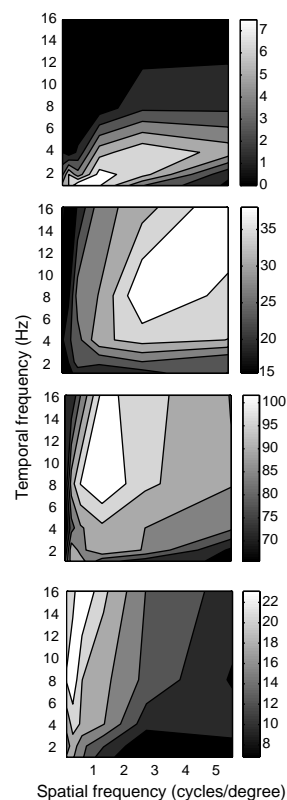
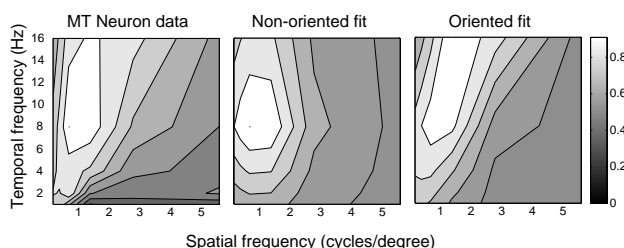


**Fig. 2.** Data from four representative MT neurons in our sample. The contour plots show the responses to sine-wave gratings moving in the neurons' preferred direction. The plots were created from the responses to 30 different grating patterns based on combinations of 6 spatial and 5 temporal frequencies (see Methods). Only the upper-right quadrant of spatiotemporal frequency space is depicted in these plots. Shaded vertical bars on right, average response of the neurons (see Methods) in each region of the plot. The regions of peak sensitivity (white) are oriented relative to the spatial and temporal frequency axes, and therefore support the oriented spectral receptive field hypothesis.



**Fig. 3.** Example of Gaussian fitting procedure. Left, response data in contour plot form from another of the MT neurons in our sample. Data are normalized relative to the maximum response across the 30 test gratings; range, 0 to 1.0 (bar on right). Middle, best-fitting non-oriented (NO) two-dimensional Gaussian (see Methods) for this cell. Right, best-fitting oriented (O) two-dimensional Gaussian. The  $(x, y)$  location of the peaks were 1.0 cycles/degree, 10.2 Hz and 1.6 cycles/degree, 13.9 Hz for the NO and O fits respectively. The  $\sigma_x, \sigma_y$  values were 1.64, 8.77 for the NO fit and 1.4, 14.4 for the O fit. The pedestal values ( $p$ ) were 0.96 (NO) and 0.88 (O). For the O fit, the value of the orientation parameter ( $\theta$ ) was  $6.5^\circ$ .



exceeded the critical level (Fig. 4). An oriented two-dimensional Gaussian provided a better description of these data than a non-oriented Gaussian. However, for a proportion of neurons (~40%), the distinction between oriented and non-oriented was not discernable, a result consistent with earlier reports of the prevalence of spectral receptive field orientation in MT (W.T. Newsome, M.S. Gizzi & J.A. Movshon, *Invest. Ophthalm. Vis. Sci. Suppl.* 29, 106, 1983; J.A. Movshon *et al.*, *Invest. Ophthalm. Vis. Sci. Suppl.* 24, 327, 1988). Possible reasons for this result are discussed below.

The spectral receptive fields of a large proportion of our MT neuron population tended to have a ridge of peak sensitivity oriented relative to the spatial and temporal frequency axes. An oriented Gaussian that is not aligned with the spatial or temporal frequency axes comes under the category of an inseparable two-dimensional function. We therefore conclude that most of our MT spectral receptive fields are better described as inseparable rather than separable. Because of the imprecision of our two-dimensional Gaussian fitting procedure (see Methods) and our limited sampling of the spatial and temporal frequency dimensions, we cannot be certain of the exact proportion of 'oriented' versus 'non-oriented' spectral receptive fields in our sample.

#### Spectral receptive field orientation and shape analysis

We next analyzed the aspect ratio ( $\sigma_y/\sigma_x$ ) and the orientation ( $\theta$ ) of the best-fitting oriented two-dimensional Gaussians, to see if they were consistent with the oriented spectral receptive field hypothesis. If the spectral receptive fields are elongated as suggested by the hypothesis, the spread of the fitted Gaussian along the  $\theta$  direction ( $\sigma_y$ ) should be larger than the spread in the  $90^\circ + \theta$  direction ( $\sigma_x$ ), that is,  $\sigma_y/\sigma_x > 1$ . Furthermore, if MT neurons possess spectral receptive fields tuned for the oriented spectra generated by moving edges, then we would expect the receptive field spectra in our contour plots to have a major axis that is rotated in a clockwise direction relative to the vertical (temporal frequency) axis (Fig. 1d). This means that the best-fitting oriented two-dimensional Gaussian should have a  $\theta$  parameter that is positive rather than zero or negative.

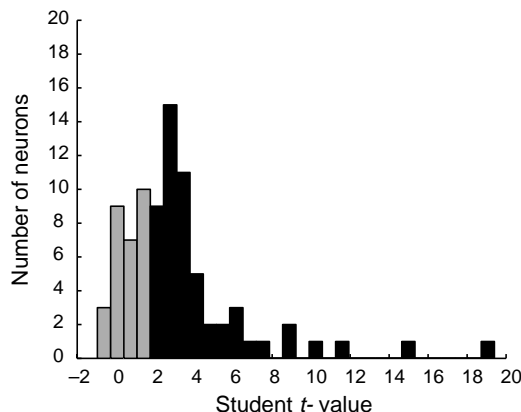
For our whole sample of MT neurons, the median value of  $\sigma_y/\sigma_x$  for the oriented two-dimensional Gaussian fits was 7.2 (mean  $\pm$  s.d.,  $26.3 \pm 69.5$ ). The  $\sigma_y/\sigma_x$  ratio for the oriented fit in Fig. 3 was 10.01. We can reject the hypothesis that the average shape of the spectral receptive fields was circular, that is,  $\sigma_y/\sigma_x = 1$  ( $t = 3.3$ ,  $df = 83$ ,  $p < 0.001$ , two-tailed). Overall, the spectral receptive fields were elongated in the direction expected by the oriented spectral receptive field hypothesis. The mean value

for the orientation parameter ( $\theta$ ) was  $6.1 \pm 8.5^\circ$ , which was significantly different from  $0^\circ$  ( $t = 6.57$ ,  $83$  *df*,  $p < 0.001$ , two-tailed).

Under the oriented spectral receptive field hypothesis, the ridges of peak sensitivity of the MT neurons' spectral receptive fields should fall on lines of different slopes passing through the origin (Fig. 5a). More formally,  $\theta$  should equal  $\beta$  in each case, where  $\beta = 90^\circ - \text{atan}(y/x)$ . Thus, ideally, the difference between  $\beta$  and  $\theta$  should equal zero. As expected, the distribution of these differences is centered around zero (Fig. 5b). The median of the error distribution was  $1.86^\circ$ , and the mean was  $5.4 \pm 14.4^\circ$ , which was significantly different from  $0^\circ$  ( $t = 3.43$ ,  $83$  *df*,  $p < 0.001$ , two-tailed). This difference can be attributed to the fact that, in many cases, the oriented two-dimensional Gaussian is not necessarily the best description of the MT neuron's spectral receptive field. The two-dimensional Gaussian function is symmetric about its main axes, and, yet, most of the spectral receptive fields we observed in our sample were asymmetric. In some cases, the oriented Gaussian fits were able to accommodate the asymmetry in the MT maps by incorporating a value of  $\theta$  that was closer to the vertical than the true orientation of the spectral receptive field. Although the oriented fits performed better than the non-oriented fits, they are still not optimal descriptors of the MT neuron spectral receptive fields, and this may be reflected in some of the  $\beta - \theta$  errors.

Examination of the  $\theta$  angle distribution in Fig. 5a reveals another difficulty we faced in attempting to verify the oriented spectral receptive field hypothesis. Most neurons (51%) had spectral receptive fields that were consistent with sensitivity to high rates of edge speed ( $> 8^\circ/s$ ). This is in keeping with earlier findings that show that MT neurons tend to be tuned to fairly high speeds<sup>15-17</sup>. It means that most MT neurons will have spectral receptive fields that have a primary orientation close to the vertical and therefore will be hard to distinguish from non-oriented spectral receptive fields. This may explain why earlier studies have reported mixed results in their search for oriented (insepa-

**Fig. 4.** Contribution of the orientation parameter ( $\theta$ ) to the two-dimensional Gaussian-MT data fits. Student  $t$ -values greater than 2.06 (black bars) indicate that the orientation parameter significantly contributed to a good fit. This was the case for most of the MT neurons (51/84 = 60.7%).



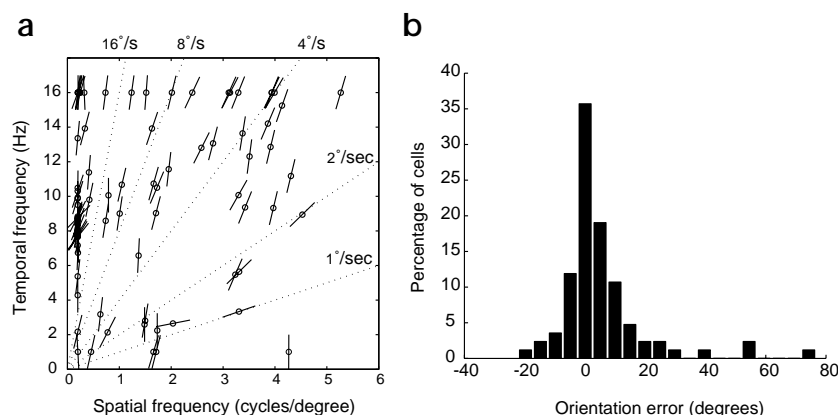


**Fig. 5.** Test of the oriented two-dimensional Gaussian alignment. **(a)** Location ( $x, y$ ) of the peaks for the best fitting oriented two-dimensional Gaussian for all cells in our sample (open circles). Lines through circles, orientation of the best-fitting Gaussian ( $\theta$ ). Dotted lines correspond to the location of the amplitude spectra that would be generated by moving edges; speeds are shown on the right and top of figure. If the oriented spectral receptive field hypothesis is true, the best-fitting Gaussians should have main axes that pass through (0, 0). **(b)** Error distribution showing how much the orientation of each best-fitting Gaussian ( $\theta$ ) deviates from the angle ( $\beta$ ) specified by the oriented spectral receptive field hypothesis. Both angles are measured from the vertical. The errors are equal to  $(\beta - \theta)$  where  $\beta = 90^\circ - \text{atan}(y/x)$ . The bin sizes are  $5^\circ$  in width. Most cells are closely aligned to the lines specified by the hypothesis.

able) fields (W.T. Newsome, M.S. Gizzi & J.A. Movshon, *Invest. Ophthalm. Vis. Sci. Suppl.* **24**, 106, 1983; J.A. Movshon *et al.*, *Invest. Ophthalm. Vis. Sci. Suppl.* **29**, 327, 1988). Fortunately, our sample included sufficient neurons tuned to slower speeds, and these helped reveal the orientation.

#### MT neuron speed responses to moving bars

Moving edges and bars have spectra containing a broad range of spatial frequencies (that is, they are 'broad-band'). The speed response of MT neurons to broad-band stimuli should therefore depend on how well the edge/bar spectrum aligns with the spectral receptive field of the neuron. In theory, neurons tuned to slow edge/bar speeds should have a shallow spectral receptive field orientation (for example, Fig. 2, top) and those tuned to higher edge/bar speeds should have a steeply oriented spectral receptive field (for example, Fig. 2, bottom). This is an obvious but critical prediction of the oriented spectral receptive field hypothesis that has never been tested experimentally before. Therefore, we measured the preferred bar speed (see Methods) along with the spatiotemporal spectral receptive fields for a subset ( $n = 48$ ) of our MT neurons.

For the four examples shown in Fig. 6, the speed tuning in response to a moving bar is closely related to the orientation of the spectral receptive field. This general trend was apparent across the subset of our MT neurons tested using moving bars (Fig. 7). The fitted line is given by  $\log V' = 0.42 \log V + 1.66$  ( $r = 0.58$ ,  $r^2 = 0.34$ ,  $F = 11.1$ ,  $1, 22 \text{ df}$ ,  $p < 0.005$ ). A lot of the noise in the data can be attributed to the fact that small errors in the  $\theta$  estimate translate into large errors in the speed estimate ( $V'$ ) because of the tangent function linking  $\theta$  and  $V'$ . This is especially so for values of  $\theta$  close to  $0^\circ$ , that is, the most common value of  $\theta$  in our sample. Overall, however, the slope of the regression line was positive. Thus, we confirm that the orientation of an MT neuron's spectral receptive field is closely tied to the optimum speed sensitivity of the neuron when tested with broad-band stimuli such as moving bars.

#### DISCUSSION

Our data show that many MT neurons have oriented (inseparable) spectral receptive fields that enable them to respond selectively to particular spatiotemporal frequency combinations, that is, to a certain speed of stimulus movement. By examining the responses of the neurons in spatiotemporal frequency space, we confirmed that these neurons have properties that are closely matched to the most common stimulus they encounter, that is, moving edges. In spatiotemporal frequency space, a moving edge has a spectrum that falls on a line oriented relative to the spatial and temporal frequency axes<sup>21,24</sup>. The elongated and oriented spectral receptive fields of the MT neurons in our sample are 'tuned' for this type of stimulus. Although it has long been suspected that this could be the case (for example, W.T. Newsome, M.S. Gizzi & J.A. Movshon, *Invest. Ophthalm. Vis. Sci. Suppl.* **24**, 106, 1983), our data provide the first clear evidence of this type of tuning.

Having demonstrated that many MT neurons possess spectral receptive fields

that are oriented and inseparable, we are still left with the question as to how these receptive fields are constructed. The neurons at an earlier stage of the visual motion pathway (V1) do not have oriented spectral receptive fields<sup>20</sup>. Yet somehow, by the time we reach MT, the neurons have acquired spectral receptive field properties that are suitable for true speed selectivity. We are currently testing our MT data against a speed mechanism model based on the combined inputs from just two V1 neurons, one with sustained temporal frequency tuning and the other with transient tuning (J.A. Perrone, *Soc. Neurosci. Abstr.* **24**, 789.9, 1998; J.A. Perrone & A. Thiele, *Invest. Ophthalm. Vis. Sci. Suppl.* **41**, S720, 2000).

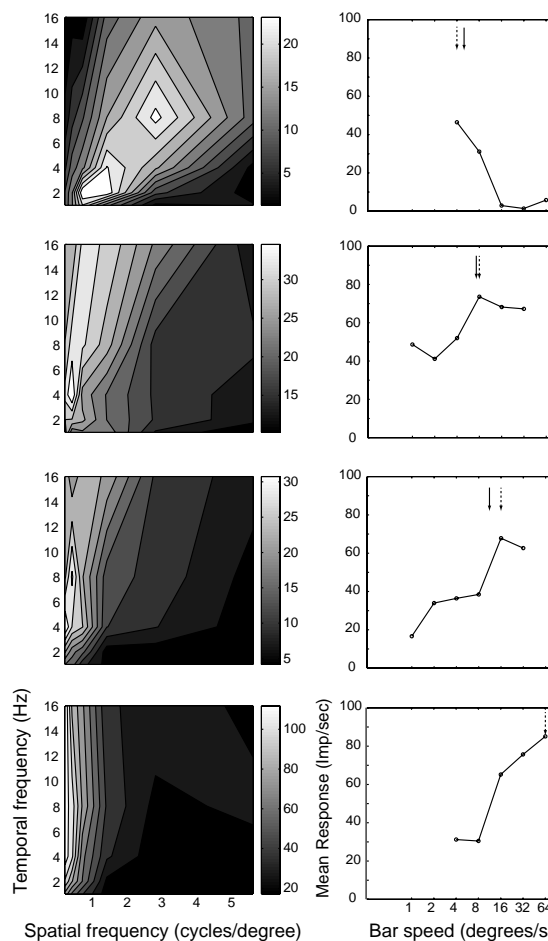
Our MT neuron data, and the earlier speed tuning results<sup>15-18</sup>, put tight constraints on theories concerning the type of speed information that is available at the level of MT. As in other domains (such as wavelength coding or direction coding), a single neuron with band-pass tuning cannot unambiguously indicate how much of a particular stimulus dimension is present. Therefore, the individual MT neurons cannot signal (for example, using a rate code) that something is moving at a particular speed (for example, 10 degrees/s). By way of illustration, as a consequence of the shape of its speed-tuning curve, the neuron in Fig. 6b would produce an output of about 70 impulses/s in response to bar speeds of both 8 and 16 degrees/s. A change in the contrast of the bar would further complicate this link between firing rate and bar speed. Therefore an estimate of the actual edge speed—presumably from some sort of population code (for example, ref. 26)—would have to be derived at a neural stage after MT. Of course, this limitation only applies to speed estimation systems based around the MT spectral receptive field properties. Visual speed estimates could also be derived by the visual system through additional means (such as feature tracking<sup>27</sup>).

The MT spectral receptive field data reported here reveal that a simple matching strategy has been adopted by the primate visual system to register the speed of moving edges. The individual spectral receptive fields act as 'templates' for a particular speed of edge movement (for example, Fig. 6). If the edge speed matches





**Fig. 6.** Relationship between the spectral receptive field orientation of representative MT neurons and their preferred speed tuning obtained from moving bar tests (see Methods). Left, spectral receptive fields from four neurons in our sample derived using moving sine-wave gratings. The orientation of the ridge of peak sensitivity relative to the spatial and temporal frequency axes was found from the  $\theta$  parameter in the best-fitting oriented two-dimensional Gaussian (see Methods). Under the oriented spectral receptive field hypothesis,  $\theta$  should be directly related to the optimum speed tuning ( $V'$ ) of the neuron, that is,  $V' = \tan(90^\circ - \theta)$  because  $V' = \text{temporal frequency/spatial frequency}$ . Solid arrows in the right panels indicate the calculated value of  $V'$ . These panels show the speed tuning curves for the same neurons obtained using a moving bar (see Methods). The dashed arrows indicate the peak of the tuning curves. From top to bottom, the peak and  $V'$  values (in degrees/s) were as follows: 4, 5.1; 8, 7.6; 16, 11.5; 64, 301 (arrow position truncated). In general, neurons with a shallow spectral receptive field slope were tuned to slow bar speeds, and those with a steep slope were tuned to high bar speeds.



the optimum speed tuning of the neuron, a large output results. If the speed is too fast or slow for the cell, the spectrum of the moving edge does not line up or match the MT spectral receptive field very well, and a low response is generated. A similar template-matching scheme seems to be at work in a motion processing area beyond MT as well. The neurons in the medial superior temporal region (MST) of primate cortex are capable of acting as templates for the global patterns of image motion that occur during self-motion<sup>5,14,28,29</sup>. The template concept is a pervasive and simple one, but in the case of MT neurons, it is not obvious that it is being applied; the nature of the neuron-stimulus match only becomes apparent in the spatiotemporal frequency domain.

#### METHODS

**Animal subjects.** We used two adult rhesus monkeys (*Macaca mulatta*, 1 male, 1 female) in this study. Experimental protocols were approved by the Salk Institute Animal Care and Use Committee, and conform to USDA regulation and to NIH guidelines for the humane care and use of laboratory animals. Details about procedures for surgery, wound maintenance and the behavioral fixation task are provided elsewhere<sup>30,31</sup>.

**Electrophysiological recordings.** Details about procedures for recording extracellular action potentials from isolated cortical neurons are routine, and have been described repeatedly elsewhere (for example, ref. 32). Four criteria were used to determine whether neurons were recorded from MT: selectivity for the direction of stimulus motion, consistency of retinotopic organization with known topography, consistency of receptive fields with known dependence on visual field eccentricity, and consistency of electrode positions (determined from activity pattern while advancing into MT) with expected sulcal topography. In addition, stereotaxic MRI scans obtained before surgery were used to further confirm that our recordings were in a region of cortex consistent with the typical location of area MT.

**Apparatus.** Visual stimuli were generated using a SGT Pepper Graphics board (Number Nine Computer Corporation, 640 × 480 pixel resolution on 27 × 20.25 cm, analog RGB output, 8 bits/gun) residing in a Pentium-based PC. Stimuli were displayed on an analog RGB monitor (Sony GDM 2000TC, 60 Hz, non-interlaced) at a distance of 63 cm. CORTEX 5.7 (Laboratory of Neuropsychology, NIMH) was used for data acquisition, behavioral control and stimulus generation. Monitor output was linearized for each of the three phosphors independently<sup>33</sup>.

**Determination of basic response properties.** Initially, each isolated MT neuron was mapped while monkeys fixated centrally. Thereafter, direction tuning was assessed using a sinusoidal grating (0.7 cycles/degree, 4 Hz, 100% Michelson contrast) moving in each of eight different directions (along cardinal and oblique axes) centered on the receptive field.

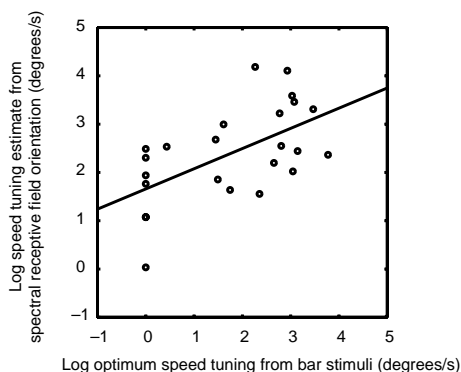


**Fig. 7.** Prediction of the spectral receptive field orientation of MT neurons from their optimum speed tuning, obtained using a moving bar. A subset (48/84) of the neurons in our sample were tested with a moving bar in addition to the standard sinusoidal grating tests. This produced speed tuning curves from which the optimum speed ( $V$ ) of the neuron was estimated by fitting a one-dimensional Gaussian to the speed tuning data (see Methods). The log-transformed  $V$  estimates have been plotted against  $\log V'$ , where  $V'$  is the speed tuning estimate based on the orientation of the spectral receptive field of the neuron (see Methods). A standard linear regression analysis was carried out to see if  $V'$  is predictable from  $V$ . This analysis was done for all neurons in our sample (24/48) that produced an oriented Gaussian fit with an  $r$ -value greater than 0.8 (the average for the non-oriented Gaussian fits) and a fit to the speed-tuning data, which also exceeded  $r = 0.8$ .



The direction of motion that yielded the largest response was termed the 'preferred' direction, and the direction opposite to the preferred was termed the 'null' direction. Strength of directional bias along the preferred-null axis was quantified by a direction index (DI):  $DI = 1 - ND/PD$ , where PD and ND are firing rate changes elicited by motion in preferred and null directions, respectively (after subtraction of background activity). Neurons with a  $DI < 0.5$  were excluded from further study, that is, all 84 neurons used in the current study were directionally selective.

**Mapping the spectral receptive field.** Stimuli consisted of moving yellow-black sinusoidal gratings with a mean luminance of  $24 \text{ cd/m}^2$ . They were presented on a yellow background ( $24 \text{ cd/m}^2$ ), with CIE coordinates  $x = 0.492$ ,  $y = 0.446$ . Stimuli were viewed within a square aperture and moved along one of the cardinal or oblique axes. Aperture width was  $5^\circ$  for neurons with foveal and parafoveal receptive fields, and  $10^\circ$  if a neuron's receptive field diameter was larger than  $5^\circ$ .

Thirty different spatiotemporal frequency combinations moving in the preferred direction were used to determine the spectral receptive field (temporal frequencies, 1, 2, 4, 8 or 16 Hz; spatial frequencies, 0.2, 0.4, 0.7, 1.4, 2.8 or 5.6 cycles/degree). Luminance modulation of sinusoidal stimuli was set to 10% Michelson contrast. The choice of a relatively low contrast resulted from initial testing with high (100%) luminance contrast. Stimuli of 100% luminance contrast activate MT neurons strongly at most spatiotemporal frequencies, thereby potentially concealing the oriented spectral receptive field. Weaker stimuli failed to activate neurons if spatiotemporal frequencies were non-optimal. The neuron's spatiotemporal frequency tuning could therefore be recovered more easily. Neuronal data were included into the sample if 5–8 trials per condition were recorded.

**Data analysis.** For each neuron, we calculated the mean activity for each stimulus condition ( $n = 30$ ) over a 1000-ms window, which began 50 ms after stimulus onset and ended 50 ms after stimulus offset. These means were then used to construct the spatiotemporal frequency tuning and plotted in contour plot form (for example, see Fig. 2). The means were normalized relative to the peak value to give a  $6 \times 5$  array of responses  $R$ . These 30 values were fitted with a two-dimensional Gaussian function:  $G(u, \omega) = (\exp(-(u')^2/\sigma_x^2)) \times (\exp(-(\omega')^2/\sigma_y^2)) + p$ , where  $u' = (u - x) \cos \theta + (\omega - y) \sin \theta$  and  $\omega' = -(u - x) \sin \theta + (\omega - y) \cos \theta$ . Here,  $u$  is the spatial frequency of the test grating,  $\omega$  is the temporal frequency,  $(x, y)$  is the location of the peak of the Gaussian (in  $u, \omega$  coordinates),  $\sigma_x$  and  $\sigma_y$  is the spread of the Gaussian in the  $u'$  and  $\omega'$  dimensions, respectively. A constant value ( $p$ ) is added, and then the  $G$  values are normalized relative to the maximum. The values of  $x, y, \sigma_x, \sigma_y$  and  $p$  were optimized using `fminsearch` in MatLab (MathWorks, Natick, Massachusetts) to minimize the sum of the squared deviations (see below) between the thirty  $R$  and  $G$  values. Two versions of the two-dimensional Gaussian were fitted: non-oriented, in which  $\theta$  was constrained to equal  $0^\circ$ , and oriented, where  $\theta$  was free to take on any value. For all neurons, the degree of fit between the final optimized Gaussian function values and the 30 MT responses was measured using the mean-squared error.

$$\frac{1}{N} \sum_{j=1}^N (R_j - G_j)^2$$

Here,  $R_j$  is the MT neuron response at spatial and temporal frequency  $(u_j, \omega_j)$ , and  $G_j$  is the value of the Gaussian model (non-oriented or oriented) at  $(u_j, \omega_j)$ . We calculated the correlation coefficient ( $r$ ) as a direct measure of the fit between the Gaussian values and the MT responses. We tested the hypothesis that  $\theta = 0^\circ$  in the oriented model case by calculating the 95% confidence intervals on the nonlinear least-squares parameter estimate of  $\theta$ . These confidence intervals can be used to derive a  $t$ -value that reflects the probability that the  $\theta$ -value significantly contributed to the fit<sup>25</sup>. This confidence interval estimation process relies, to a certain extent, on the assumption of equal variance across the  $R_j$  values. However, it has been repeatedly reported that the standard variation of MT responses (the variance) scales linearly with the mean (for example, ref. 34). We therefore tested the robustness of our approach by repeating the non-linear regression analysis after we had first transformed all of the  $R_j$  responses using a square-root transform. The distribution of  $t$ -values was largely unaffected by this transformation, and the pro-

portion of neurons for which we were able to reject the  $\theta = 0^\circ$  hypothesis remained about the same (62% transformed, 61% non-transformed).

**Speed tuning tests with moving bars.** A bar  $10^\circ$  long and  $0.2^\circ$  or  $0.5^\circ$  wide (depending upon size of receptive field) was moved in the preferred direction of the cell. Its main axis was orthogonal to this direction and had a mean luminance of  $22.8 \text{ cd/m}^2$ . (That is, the Michelson contrast was 10%.) We explored various speed ranges during the course of the study to try to improve the likelihood of including the 'peak' in the speed tuning curves. For 11 of our neurons, the bar speeds were 4, 8, 16, 32 and  $64^\circ/\text{s}$ . For 15 neurons, the test speeds were 1, 2, 4, 8, 16 and  $32^\circ/\text{s}$ . One neuron was tested at 1, 2, 4, 8, 16, 24, 32, 48 and  $56^\circ/\text{s}$ , and the remainder (21) were tested at 1, 2, 4, 8, 16, 24, 32, 40, 48 and  $56^\circ/\text{s}$ . Because the refresh rate of our monitor was limited to 60 Hz, the problem of temporal aliasing<sup>23</sup> was a concern, so we treated the data generated from the higher speeds with caution. Most neurons had a peak that was clearly defined without reliance on the high speed ( $56^\circ/\text{s}$ ,  $64^\circ/\text{s}$ ) data. Usually, 5–8 trials were recorded at each speed with each trial lasting 1000 ms. The bar started moving from a position that ensured that it was at the center of the receptive field 500 ms after the start of trial. Care must be taken in selecting an appropriate response measure when testing neurons for speed selectivity using non-periodic stimuli such as bars or edges<sup>17,35</sup>. Because the bar always crossed the center of the receptive field at a known time, we averaged the responses over a fixed time window (200 ms long) and with a constant lag (50 ms) relative to the 500 ms mark. The mean responses to each bar speed were then fit with a one-dimensional Gaussian for which the amplitude, mean, standard deviation and a pedestal value were optimized to produce the best fit (in a minimum least-squares sense). The mean of the Gaussian ( $V$ ) was taken as an estimate of the speed tuning preference of the neuron. In the fitting procedure,  $V$  was constrained to lie between 1 and  $64^\circ/\text{s}$  (the maximum range of our bar test speeds). The 'peaks' derived from the Gaussian fitting nearly all lay within the range of bar test speeds. Only two neurons in our regression analysis (Fig. 7) had a mean  $V$  lower than the minimum bar speed at which the neuron was tested at ( $4^\circ/\text{s}$ ). A correlation coefficient ( $r$ ) was used to assess the degree of fit. Speed tuning estimates were not derived for neurons where the Gaussian fit produced  $r$  values less than 0.8.

#### ACKNOWLEDGEMENTS

We thank K. Dobkins, R. Krauzlis and G. Stoner for their comments, and J. Costanza and K. Sevenbergen for technical assistance. This work was supported by NASA grant NAG 2-1168 to J.P. and a Human Frontier Science Program fellowship to A.T. Some of the research reported in this paper was done during tenure by J.P. as a Sloan Visiting Scientist at the Salk Institute.

RECEIVED 28 NOVEMBER 2000; ACCEPTED 16 MARCH 2001

- Gibson, J. J. *The Perception of the Visual World* (Houghton Mifflin, Boston, 1950).
- Nakayama, K. Biological image motion processing: a review. *Vision Res.* 25, 625–660 (1984).
- Koenderink, J. J. & van Doorn, A. J. Invariant properties of the motion parallax field due to the movement of rigid bodies relative to the observer. *Opt. Acta.* 22, 773–791 (1975).
- Longuet-Higgins, H. C. & Prazdny, K. The interpretation of moving retinal images. *Proc. R. Soc. Lond. B Biol. Sci.* 208, 385–397 (1980).
- Perrone, J. A. & Stone, L. S. A model of self-motion estimation within primate extrastriate visual cortex. *Vision Res.* 34, 2917–2938 (1994).
- Dubner, R. & Zeki, S. M. Response properties and receptive fields of cells in an anatomically defined region of the superior temporal sulcus. *Brain Res.* 35, 528–532 (1971).
- Maunsell, J. H. R. & Newsome, W. T. Visual processing in monkey extrastriate cortex. *Annu. Rev. Neurosci.* 10, 363–402 (1987).
- Adelson, E. H. & Movshon, J. A. Phenomenal coherence of moving visual patterns. *Nature* 300, 523–525 (1982).
- Albright, T. D. Direction and orientation selectivity of neurons in visual area MT of the macaque. *J. Neurophysiol.* 52, 1106–1129 (1984).
- Stoner, G. R. & Albright, T. D. Neural correlates of perceptual motion coherence. *Nature* 358, 412–414 (1992).
- Newsome, W. T., Britten, K. H. & Movshon, J. A. Neuronal correlates of a perceptual decision. *Nature* 341, 52–54 (1989).
- Newsome, W. T., Wurtz, R. H., Dürsteler, M. R. & Mikami, A. Deficits in visual motion processing following ibotenic acid lesions of the middle temporal visual area of the macaque monkey. *J. Neurosci.* 5, 825–840 (1985).



13. Lisberger, S. G. & Movshon, J. A. Visual motion analysis for pursuit eye movements in area MT of macaque monkeys. *J. Neurosci.* **19**, 2224–2246 (1999).
14. Tanaka, K. & Saito, H. Analysis of the motion of the visual field by direction, expansion/contraction, and rotation cells clustered in the dorsal part of the medial superior temporal area of the macaque monkey. *J. Neurophysiol.* **62**, 626–641 (1989).
15. Maunsell, J. H. R. & Van Essen, D. C. Functional properties of neurons in the middle temporal visual area of the macaque monkey. I. Selectivity for stimulus direction, speed, orientation. *J. Neurophysiol.* **49**, 1127–1147 (1983).
16. Lagae, S., Raiguel, S. & Orban, G. A. Speed and direction selectivity of macaque middle temporal neurons. *J. Neurophysiol.* **69**, 19–39 (1993).
17. Rodman, H. R. & Albright, T. D. Coding of visual stimulus velocity in area MT of the macaque. *Vision Res.* **27**, 2035–2048 (1987).
18. Felleman, D. J. & Kaas, J. H. Receptive-field properties of neurons in the middle temporal visual area (MT) of owl monkeys. *J. Neurophysiol.* **52**, 488–513 (1984).
19. Orban, G. A., Kennedy, H. & Bullier, J. Velocity sensitivity and direction selectivity of neurons in areas V1 and V2 of the monkey: Influence of eccentricity. *J. Neurophysiol.* **56**, 462–480 (1986).
20. Foster, K. H., Gaska, J. P., Nagler, M. & Pollen, D. A. Spatial and temporal frequency selectivity of neurones in visual cortical areas V1 and V2 of the macaque monkey. *J. Physiol. (Lond.)* **365**, 331–363 (1985).
21. Watson, A. B. & Ahumada, A. J. in *Motion: Perception and Representation* (ed. Tsotsos, J. K.) 1–10 (Association for Computing Machinery, New York, 1983).
22. Bracewell, R. N. *The Fourier Transform and its Applications* (McGraw-Hill, New York, 1978).
23. Watson, A. B., Ahumada, A. J. Jr. & Farrell, J. E. Window of visibility: a psychophysical theory of fidelity in time-sampled visual motion displays. *J. Opt. Soc. Am. A* **3**, 300–307 (1986).
24. Fahle, M. & Poggio, T. Visual hyperacuity: spatiotemporal interpolation in human vision. *Proc. R. Soc. Lond. B Biol. Sci.* **213**, 451–477 (1981).
25. Draper, N. R. & Smith, H. *Applied Regression Analysis* (Wiley-Interscience, New York, 1998).
26. Treue, S., Hol, K. & Rauber, H. J. Seeing multiple directions of motion-physiology and psychophysics. *Nat. Neurosci.* **3**, 270–276 (2000).
27. Del Viva, M. M. & Morrone, M. C. Motion analysis by feature tracking. *Vision Res.* **38**, 3633–3653 (1998).
28. Perrone, J. A. Model for the computation of self-motion in biological systems. *J. Opt. Soc. Am. A* **9**, 177–194 (1992).
29. Perrone, J. A. & Stone, L. S. Emulating the visual receptive field properties of MST neurons with a template model of heading estimation. *J. Neurosci.* **18**, 5958–5975 (1998).
30. Dobkins, K. R. & Albright, T. D. What happens if it changes color when it moves?: The nature of chromatic input to macaque visual area MT. *J. Neurosci.* **14**, 4854–4870 (1994).
31. Thiele, A., Dobkins, K. R. & Albright, T. D. The contribution of color to motion processing in macaque middle temporal area. *J. Neurosci.* **19**, 6571–6587 (1999).
32. Thiele, A., Distler, C. & Hoffmann, K. P. Decision related activity in the macaque dorsal visual pathway. *Eur. J. Neurosci.* **11**, 2044–2058 (1999).
33. Watson, A. B. *et al.* Use of a Raster framebuffer in vision research. *Behav. Res. Meth. Instr. Comp.* **18**, 587–594 (1986).
34. Britten, K. H., Shadlen, M. N., Newsome, W. T. & Movshon, J. A. Responses of neurons in macaque MT to stochastic motion signals. *Vis. Neurosci.* **10**, 1157–1169 (1993).
35. Movshon, J. A. The velocity tuning of single neurons in the striate cortex. *J. Physiol. (Lond.)* **249**, 445–468 (1975).